Food and Chemical Toxicology 128 (2019) 119–128

Contents lists available at ScienceDirect

Food and Chemical Toxicology

journal homepage: www.elsevier.com/locate/foodchemtox

Chemistry and immunostimulatory activity of a polysaccharide from *Undaria pinnatifida*

Yongyi Yu[a,b,1], Yajun Zhang[a,b,1], Cebin Hu[a,b], Xinyuan Zou[a,b], Yang Lin[a,b], Yangyuan Xia[a,b], Lijun You[a,b,*]

[a] School of Food Science and Engineering, South China University of Technology, Guangzhou, Guangdong, 510640, People's Republic of China
[b] Overseas Expertise Introduction Center for Food Nutrition and Human Health (111 Center), Guangzhou, 510640, People's Republic of China

ARTICLE INFO

Keywords:
Undaria pinnatifida
Polysaccharide
RAW264.7 cell
Immunomodulatory activity
Structure

ABSTRACT

An immunologically active polysaccharide named as UPP-2 (1035.52 kDa) was isolated from *Undaria pinnatifida* using traditional water extraction followed by DEAE Sepharose fast flow chromatography. UPP-2 was proven to be a low sulfated polysaccharide with relatively abundant uronic acid (13.08 ± 0.67%). UPP-2 mainly consisted of xylose (64.55%), glucose (23.81%), arabinose (5.90%) and mannose (4.26%), and its main glycosidic linkage types included →2)-α-D-Xylp-(1→, →4)-α-D-Glcp-(1→, α-D-Xylp-(1→ and →2,4)-β-D-Xylp-(1→. Results indicated that UPP-2 significantly promoted the proliferation and pinocytic capacity of RAW264.7 cells, and up-regulated the mRNA expressions of iNOS, TNF-α, IL-6 and IL-1β at 100–600 μg/mL with a maximum of 195, 42, 768 and 539 times of those of the negative control, respectively. Moreover, UPP-2 significantly increased the secretions of nitric oxide, TNF-α and IL-6 at 100–600 μg/mL (8.0, 73.1 and 188.7 times compared to those of the negative control, respectively), as well as promoted the production of IL-1β obviously at 600 μg/mL. Overall, UPP-2 could be served as a potential dietary supplement or functional food based on its immunostimulatory activity.

1. Introduction

As an important source of dietary fibers, edible seaweeds not only play important roles in human healthy diet, but also can be considered as a good source for functional foods. *Undaria pinnatifida*, a temperate brown seaweed contains carbohydrates, proteins, volatile oils, unsaturated fatty acids, carotenoid metabolites and other chemical constituents, is widely distributed and used in east Asia, Australia and other countries. It was reported to be treated as a traditional Chinese medicine as well as a functional food source in China (Han et al., 2016).

According to previous studies, polysaccharides from *U. pinnatifida* exhibited good biological activities, such as antitumor activity (Han et al., 2016; Vishchuk et al., 2013), antiviral activity (Kim et al., 2017), antioxidant activity (Phull et al., 2017), and anticoagulant activity (Faggio et al., 2015). A previous study has explored the immunomodulatory effects of *U. pinnatifida* polysaccharides in dendritic cells, natural killer cells and T cells (H. Zhang et al., 2015a,b). Nevertheless, studies of polysaccharides from *U. pinnatifida* mainly focused on antitumor and antiviral activities, and their potential immunomodulatory activities have not attracted necessary attention. Besides, there are few reports on the structure of polysaccharides from *U. pinnatifida*, which may delay the development of *U. pinnatifida*.

Macrophages exert important roles in both innate and adaptive immunity of vertebrates for their functions of antigen presentation, phagocytosis and pinocytosis, and cytokine secretion. Macrophages are also effector cells to fight against infection and inflammation (Yan et al., 2018). As a family member of macrophages, murine RAW264.7 cells have been favored by many scientific researchers and widely used in the studies of immune activity. Recently, immunomodulatory effects of polysaccharides from *Amillariella mellea*, *Dendrobium devonianum*, *Agaricus brasiliensis*were evaluated by using RAW264.7 macrophages model (Deng et al., 2018; Yan et al., 2018; Zhang et al., 2018).

In the present work, a sulfated polysaccharide designated as UPP-2 was obtained from *U. pinnatifida*. The immunomodulatory activity of UPP-2 was evaluated by using a murine RAW264.7 macrophages model. In addition, the primary chemical composition and structural characteristics of UPP-2 were studied. The relationship between the

* Corresponding author. School of Food Science and Engineering, South China University of Technology, 381 Wushan Road, Guangzhou, Guangdong, 510640, People's Republic of China.
E-mail address: feyoulijun@scut.edu.cn (L. You).
[1] These two authors contributed equally to this article.

https://doi.org/10.1016/j.fct.2019.03.042
Received 10 December 2018; Received in revised form 12 March 2019; Accepted 21 March 2019
Available online 26 March 2019
0278-6915/

immunostimulatory activity of UPP-2 and its chemical structure was also discussed.

2. Materials and methods

2.1. Materials and chemicals

Undaria pinnatifida was collected from a local market of Weihai, Shandong, China. RAW264.7 cells from murine were acquired from ATCC (Rockville, USA). Diethylaminoethyl (DEAE)-Sepharose fast flow was acquired from GE Healthcare (Uppsala, Sweden). BCA protein assay kit was purchased from Beyotime Biotechnology Co., Ltd. (Jiangsu, China). Curdlan, rhamnose, arabinose, fucose, xylose, mannose, glucose, galactose, galacturonic acid and lipopolysaccharide (LPS) were purchased from Sigma-Aldrich, Ltd. (St. Louis, MO, USA). Sodium borohydride, inositol, glycerol and erythritol were obtained from Aladdin Biochemical Technology Co., Ltd. (Shanghai, China). Dulbecco's modified eagle's medium (DMEM), fetal bovine serum (FBS), streptomycin, penicillin and Hank's balanced salt solution (HBSS) were purchased from Gibco Biotechnology Co., Ltd. (Grand Island, NY, USA). Limulus reagent (0.5 EU/mL) was purchased from Xiamen Bioendo Technology Co., Ltd. (Xiamen, China). Total RNA extraction kit and the reverse transcription (RT) kit with gDNA eraser were purchased from Dongsheng Biotech Co., Ltd (Guangzhou, China) and Takara Biomedical Technology Co., Ltd. (Beijing, China), respectively. Forward/reverse primers were provided by Sangon Biotech Co., Ltd. (Shanghai, China). The iTaq < SUP > TM < /SUP > Universal SYBR® Green Supermix was purchased from Bio-Rad Laboratories, Inc. (Hercules, USA). Griess reagent, sodium nitrite, alcohol, gelatin, neutral red and Congo red reagent were purchased from Guangzhou Reagent Co. (Guangzhou, China). The mouse TNF-α, IL-6 and IL-1β ELISA kits were purchased from Neobioscience Technology Co., Ltd. (Shenzhen, China).

2.2. Extraction, purification of polysaccharides from U. pinnatifida

U. pinnatifida was rinsed and dried up in an oven at 60 °C, then crushed into powder using a grinder (FW135, Taisite, Tianjin, China) and filtered with a 0.45 mm mesh. To decolor and remove alcohol-soluble chemicals, the powder was mixed with ethanol at a ratio of 1:4 (w/v, g/mL) and kept a slight boiling in a reflux device for 3 h, then the residue was dried up at 60 °C.

Polysaccharides from *U. pinnatifida* was extracted by traditional hot water extraction. Briefly, 25 g of *U. pinnatifida* powder was added to 1000 mL distilled water followed by a 4 h extraction at 100 °C, then the mixture was centrifuged at 5000 rpm, 25 °C for 10 min (Allegra X-15R, Beckman Coulter, USA). The supernatant obtained was concentrated to 1/4 of its original volume at 60 °C by a reduced rotary evaporator (HeiVAP Value Digital, Heidoph, Germany), after which 4 times the volume of ethanol was added and incubated for overnight at 4 °C. Then the residue obtained by centrifugation were collected, redissolved and lyophilized. Finally the crude polysaccharide named as UPP was obtained and stored at −20 °C until use.

DEAE Sepharose fast flow chromatography was applied to the purification of UPP. Briefly, UPP (75 mg) was dissolved in 2 mL distilled water and loaded onto a DEAE Sepharose fast flow column (20 mm × 60 cm), then successively eluted with NaCl solutions of different concentrations (0–0.8 M) at a flow rate of 1.83 mL/min. The obtained eluent fractions were concentrated at 60 °C and then analyzed using the phenol-sulfuric acid method (Dubois et al., 1951). Then four carbohydrate-abundant fractions were obtained and dialyzed against deionized water (Mw cut off 3000 Da) in dialysis bags for 48 h at 4 °C, the resultant solution was then freeze-dried. Finally, four fractions, eluted by 0, 0.2, 0.3 or 0.4 M NaCl solutions, were obtained and named as UPP-1, UPP-2, UPP-3 and UPP-4, respectively. The present study focused on UPP-2 for its strongest potential immunostimulatory activity based on the previous study of its promotion effect on NO release (data not shown).

2.3. Chemical composition determination of UPP-2

The total carbohydrate content of UPP-2 was determined using phenol-sulfuric acid method (Dubois et al., 1951); the sulfate and uronic acid contents of UPP-2 were determined by barium sulfate turbidity method and the carbazole colorimetry method reported by Zhang et al. (2015) and Bitter et al. (1962), respectively. The protein content was determined by using a BCA protein assay kit, and the total phenolic content was determined by the modified Folin-Ciocalteu method (Singleton et al., 1999). Endotoxin test was carried out by guideline of the limulus reagent kit.

2.4. Ultraviolet rays (UV) spectrum analysis of UPP-2

The UV spectrum of UPP-2 was performed by a Nucleic acid/Protein analyzer (Du 730, Beckman Coulter, USA) at a wavelength range of 200–400 nm.

2.5. Structural characterization of UPP-2

2.5.1. Determination of molecular weight

The molecular weight (Mw) of UPP-2 was determined using a high performance gel permeation chromatography (HPGPC) equipped with an Agilent G-5000 PWXL column (7.8 × 300 mm i.d., 10 μm), a G-3000 PWXL column (7.8 × 300 mm i.d., 5 μm), as well as an Agilent 1260 refractive index detector. UPP-2 (2 mg) was dissolved in 1 mL of 0.02 M KH_2PO_4 solution and filtered through a 0.22 μm organic membrane, then the filtrate was loaded onto an analytical column with an injection volume of 20 μL and eluted with 0.02 M KH_2PO_4 solution at a flow rate of 0.6 mL/min. Dextran with different molecular weight (6000–2500000 Da) were used as the standard to obtain the calibration curve of Mw.

2.6. Infrared spectrum (IR) analysis

After mixed with KBr, UPP-2 (2 mg) was pressed into thin slices, then the scan test was performed at a wavelength of 400–4000 cm^{-1} using a Vector 33 FT-IR spectrometer (Bruker, Ettlingen, Germany).

2.6.1. Triple-helix structureanalysis

The conformational structure analysis of UPP-2 was performed according to the Congo red method reported by Ji et al. (2017). Curdlan with triple helical conformation was used as a positive control.

2.6.2. Determination of monosaccharide composition

Monosaccharide composition of UPP-2 was determined by gas chromatography (GC) method with precolumn derivatization. Briefly, UPP-2 (10 mg) was fully hydrolyzed by 5 mL of 4 M trifluoroacetic acid (TFA) at 110 °C for 6 h, then TFA was removed at 60 °C using a rotary evaporator, after which the residue was mixed with 2 mL of methanol and dried up at 45 °C by a nitrogen blow concentrator. Then, hydroxylamine hydrochloride (10 mg) and 2 mL pyridine were added, followed by a reaction at 90 °C for 30 min. The resultant product was then acetylated by acetic anhydride (2 mL) at 90 °C for 30 min. The acetylated monosaccharides were extracted by dichloromethane and filtered through a 0.22 μm organic membrane. Finally, the samples were analyzed by GC with a HP-5MS column (30 m × 0.25 mm × 0.25 μm, Agilent, USA) and a flame ionization detector. The gradient program was set as follows: The inlet temperature was 250 °C.With an initial temperature of 140 °C (held for 1 min), the column temperature was raised to 220 °C at 2 °C/min and held for 1 min, then raised to 250 °C at 10 °C/min and held for 2 min. With an injection volume of 1 μL, samples were eluted with helium (He) at a flow rate of 1.0 mL/min and a split ratio of 10:1. Arabinose, rhamnose, fucose, mannose, glucose, galactose

and xylose were used as standards.

2.7. Periodate oxidation and smith degradation analysis

Periodate oxidation-Smith degradation analysis of UPP-2 was performed by the method reported previously (Xu et al., 2012; Ye et al., 2018). Briefly, UPP-2 (20 mg) was dissolved in 12.5 mL distilled water. After mixed with 12.5 mL of 30 mM $NaIO_4$ solution, the solution was kept in darkness at room temperature. The reactant (0.1 mL) was taken out and diluted to 100 mL every 12 h, and read at 223 nm until the absorbance value was stable. The periodate oxidation was stopped by 1.5 mL glycol. The consumption of periodate was calculated according to a $NaIO_4$ standard curve with concentration proportional to optical densities in the wavelength of 223 nm. To calculate the HCOOH production, the resultant solution (2 mL) was taken out and titrated by 0.01 M NaOH standard solution. The rest solution was dialyzed against deionized water for 48 h at 4 °C followed by concentration. To destroy the furfural, sodium borohydride (70 mg) was added. After reacting for 24 h, the solution was adjusted to pH 7 by 50% acetic acid, then dialyzed against deionized water for another 48 h at 4 °C. The resultant solution was concentrated and the residue was then hydrolyzed by TFA, acetylated by acetic anhydride and extracted by dichloromethane using the method described in section 2.5.4. Finally, the samples were analyzed by GC with same chromatographic conditions as described in section 2.5.4.

2.8. Methylation analysis

Methylation analysis of UPP-2 was carried out by the method reported previously with some modifications (Lin et al., 2012). Briefly, UPP-2 (5 mg) was dissolved in 5 mL DMSO and sonicated for 2 h, then 200 mg NaOH was added followed by 30 min of sonication. Methyl iodide (2 mL) was added and the mixture was kept stirring in darkness for 1 h, then dried up by a nitrogen blow concentrator. Another 2 mL of methyl iodide was added again, and this procedure was repeated three times. While for the last addition of methyl iodide, the mixture was kept stirring in darkness for 24 h, then 4 mL distilled water was added to stop the methylation reaction. The methylated polysaccharide was extracted by 4 mL chloroform and purified by 4 mL distilled water (repeat the operation five times). Then the methylated product was hydrolyzed, acetylated and extracted as described in section 2.5.4. Finally, the samples were analyzed by a gas chromatography-mass spectrometer (GC-MS, 6890-5975i, Agilent, USA) equipped with an Agilent HP-5MS column (30 m × 0.25 mm × 0.25 μm). The gradient program was set as follows: The inlet temperature was 250 °C. With an initial temperature of 150 °C (held for 2 min), the column temperature was raised to 180 °C at 10 °C/min and held for 2 min, then raised to 260 °C at 15 °C/min and held for 5 min. With an injection volume of 1 μL, samples were eluted with helium (He) at a flow rate of 1.0 mL/min.

2.8.1. NMR spectroscopy analysis

The ^{1}H NMRand ^{13}C NMR spectroscopy analysis of UPP-2 (50 mg/mL dissolved in D_2O) were performed by a 600 MHz NMR analyzer (Bruker Corp, Fallanden, Switzerland).

2.9. Immunostimulatory activity analysis of UPP-2

2.9.1. Cytotoxicity assay

RAW264.7 cells were cultured in DMEM medium (glucose content < 1000 mg/L) added with FBS (10%, v/v), streptomycin (100 μg/mL) and penicillin (100 units/mL) in a cell incubator at 37 °C with 5% CO_2. Cells in log phase were treated with trypsin and seeded on 96-wellplates with a total of 1.5×10^4 cells/well. After incubating for 24 h, the growth medium was removed and 100 μL fresh medium with different concentrations (50–1000 μg/mL) of UPP-2 or LPS (150 ng/mL) were added. After incubating for another 24 h, the growth medium was removed and the cells were washed by PBS twice, then 50 μL of methylene blue solution (HBSS + 0.6% methylene blue + 1.25% glutaraldehyde) was added. After incubating for 1 h, the cells were washed by PBS for three times. Subsequently, elution solution (100 μL) with 50% of ethanol, 49% of PBS and 1% of acetic acid were added. The absorbance at 570 nm was measured by a microplate reader (FilterMax F5, Molecular Devices, USA).

2.9.2. Determination of pinocytic capacity of RAW264.7 cells

The pinocytic capacities of RAW264.7 cells treated with UPP-2 or LPS were determined using the reported method with minor modification (Yu et al., 2017). RAW 264.7 cells in log phase were seeded on a 96-well plate with a total of 1.5×10^4 cells/well and incubated for 24 h. Then the growth medium was replaced by fresh medium with UPP-2 at different concentrations or LPS. After incubating for 24 h, the growth medium was replaced by 100 μL of 0.075% neutral red in PBS. The cells were washed for several times after an incubation of 3 h, and 100 μL elution solution was then added to each well. Finally the absorbance at 540 nm was measured by a microplate reader (FilterMax F5, Molecular Devices, USA). The pinocytic capacities of cells in experimental groups were compared to that of the control group based on the absorbance values.

2.9.3. Reverse transcription-quantitative real-time PCR (RT-QPCR) assay

After treated with UPP-2 at different concentrations (100–600 μg/mL) in DMEM medium for 24 h, RAW264.7 cells were trypsinized and collected for the isolation of total RNA using a RNA extraction kit. Then the total RNA was reversed using a RT kit with gDNA eraser. Finally, the quantification of the cDNA encoding iNOS, IL-6、IL-1β and TNF-α was performed by quantitative real-time PCR assay using iTaq Universal SYBR Green Supermix as quantitative enzyme, and Finally the calculation of relative gene expression level were carried out by the method reported by Livak et al. (2001). GADPH was set as the internal reference.

The specific primers and their sequencesused were listed as follows: GADPH-Forward (F) 5′-TTTGTCAAGCTCATTTCCTGGATATG-3′, GADPH-Reverse (R) 5′-TGGGATAGGGCCTCTCTTGC-3’; iNOS-F 5′-CGGCAAACATGACTTCAGGC-3′, iNOS-R 5′-GCACATCAAAGCGGCCATAG-3’; TNF-α-F 5′-GGGGATTATGGCTCAGGGTC-3′, TNF-α-R 5′-CGAGGCTCCAGTGAATTCGG-3’; IL-6-F 5′-TACTCGGCAAACCTAGTGCG-3′, IL-6-R 5′-GTGTCCCAACATTCATATTGTCAGT-3’; IL-1β-F 5′-GAGCCTGTGTTTCCTCCTTG-3′, IL-1β-R 5′-TCCAAGAAACCATCTGGCTAGG-3’.

2.9.4. Determination of NO produced by RAW264.7 cells

Determination of NO produced by RAW264.7 cells was carried out by the method reported preciously (Ren et al., 2017), and the Griess method reported by (Shen et al., 2016) was used. After incubating for 24 h, RAW264.7 cells (1.5×10^4 cells/well) in a 96-well plate were treated with UPP-2 at different concentrations (100–600 μg/mL) or LPS (150 ng/mL) and incubated for 24 h continually. Subsequently, supernatant medium (80 μL) in each well was mixed with 40 μL Griess reagent A followed by an incubation of 10 min in darkness, Griess reagent B was then added for another incubation of 10 min. Finally, the absorbance at 540 nm was measured and the NO production was calculated according to a standard curve using $NaNO_2$ as the standard.

2.9.5. Determination of cytokines produced by RAW264.7 cells

RAW264.7 cells were cultured in 6-well plates (3×10^5 cells/well) and treated with UPP-2 or LPS for 24 h, then the levels of cytokines including IL-6, IL-1β and TNF-α in the culture medium were tested by corresponding ELISA kits.

2.10. Statistical analysis

Statistical analysis was performed by IBM SPSS 22 statistical

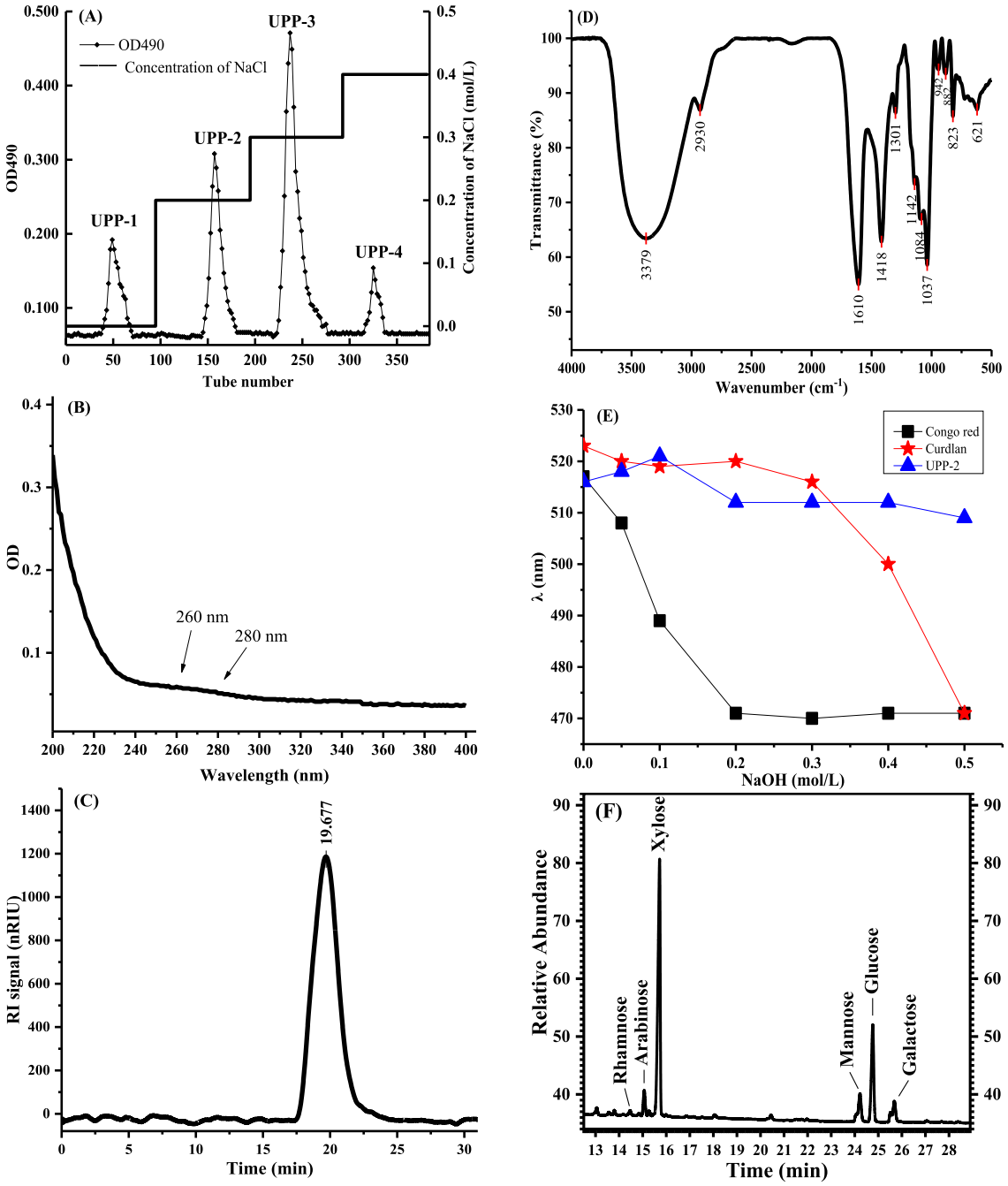

Fig. 1. DEAE chromatography elution curve of UPP (A); UV spectrum of UPP-2 (B); Molecular weight distribution of UPP-2 (C); IR spectra of UPP-2 (D); Helix-coil transition analysis of UPP-2 and Curdlan (E); Gas chromatogram of UPP-2 (F).

software (IBM Corp., Armonk, NY, USA). Data between the experimental groups were compared by one-way ANOVA, and $p < 0.05$ or $p < 0.01$ was considered to be statistically significant or extremely significant. All data were presented as mean ± standard deviation (SD) for replicate analysis (n ≥ 3).

3. Results and discussion

3.1. Yield and chemical characteristics of UPP-2

Crude polysaccharide named as UPP was isolated from *U. pinnatifida* with a yield of 11.00 ± 0.25% based on dried weight. The total sugar, sulfate and uronic acid content of UPP were 50.02 ± 1.14%, 11.19 ± 0.40% and 14.98 ± 0.52%, respectively. Purified by DEAE Sepharose fast flow chromatography (Fig. 1A), UPP was separated to 4 fractions named as UPP-1, UPP-2, UPP-3 and UPP-4 with a total recovery yield of 54.58%. UPP-2, a white flocculus-like polysaccharide which was eluted by 0.2 M NaCl solution, accounted for 16.17% of UPP. Results showed that the total sugar, sulfate, uronic acid and protein content of UPP-2 were 79.93 ± 2.07%, 6.42 ± 0.13%, 13.08 ± 0.67% and 1.42 ± 0.13%, respectively, and no polyphenols were detected. The low protein content of UPP-2 was also evidenced by its UV spectrum in a wavelength range of 200–400 nm (Fig. 1B). The limulus reagent (0.5 EU) reaction result indicated that the endotoxin content of UPP-2 was lower than the detection limit.

The data above demonstrated that UPP-2 was a low sulfated polysaccharide with relatively abundant of uronic acid. While the sulfation level of polysaccharides was reported to be related to their antioxidant

activities (Ngo and Kim, 2013). And sulfated polysaccharides from algae were reported to have potential applications in the stimulation of immune responses (Jiao et al., 2011). Besides, the uronic acid level was contributed to the hydroxyl radical scavenging activity of fucoidan from *Sargassum* sp.(Hifney et al., 2016).

3.2. Structural characteristics of UPP-2

3.2.1. Molecular weight distribution of UPP-2

Referring to the method reported by Zhang et al. (2018), a standard curve of Mw based on the logarithm of Mw (LogMw) versus retention time (T) was established as LogMw = −0.2203T + 10.35, R^2 = 0.997. A single, symmetrical peak at 19.677 min in the HPGPC spectrogram (Fig. 1C) indicated that UPP-2 was homogeneous with an average Mw of 1035.52 kDa. The Mw of polysaccharides from *U. pinnatifida* were previously reported as 97.9 kDa, 9 kDa, 582.51 kDa, 767.18 kDa or 390.58 kDa (Han et al., 2016; Song et al., 2015; Synytsya et al., 2014), which were obviously different with that of UPP-2.

3.2.2. FT-IR spectrum of UPP-2

The infrared spectra of UPP-2 showed typical absorptions of carbohydrates (Fig. 1D). The broad and strong peak at 3379 cm^{-1} was corresponding to O-H stretching vibration (Jin et al., 2015). The obvious absorptions at 2930 cm^{-1} and 1301 cm^{-1} indicated the presence of stretching and bending vibration of C-H, respectively. The bond around 1418 cm^{-1} was attributed to C-O stretching vibration. The bond at 1610 cm^{-1} corresponding to the asymmetric stretching vibration of C=O indicated the possible presence of uronic acid (Manrique and Lajolo, 2002). The absorptions at 823 cm^{-1} and 1037 cm^{-1} were due to the stretching vibrations of C-O-S and C-C, respectively (Lucassen et al., 1998). The weak peak at 1142 cm^{-1} was a characteristic absorption of pyranose, resulting from C-O-C linkage (Li et al., 2015). And the bond at 942 cm^{-1} was a characteristic absorption of β-glycosidic bond (Liang et al., 2011), while the peak at 882 cm^{-1} was a characteristic absorption of β-pyranose due to the C-H vibration.

3.2.3. Conformational structure analysis

The conformational analysis of UPP-2 was carried out by the Congo red method. As shown in Fig. 1E, curdlan with triple-helix structure caused an obvious red-shift of 6 nm in maximum absorption wavelength when complexed with Congo red. With the increase of NaOH concentration, the maximum absorption wavelength of the curdlan-Congo red solution decreased slightly first, and then began to decrease sharply when NaOH concentration reached 0.3 M, indicating that the triple-helix structure of curdlan was destroyed. Nevertheless, UPP-2 didn't exhibit a triple-helix structure for neither a red-shift nor an obvious decrease of maximum absorption wavelength.

3.2.4. Monosaccharide composition of UPP-2

To determine the monosaccharide composition of UPP-2, its hydrolyzed and acetylated products were analyzed by GC. Acetylated products of seven monosaccharide standards were diluted to series of molar concentrations followed by GC analysis for qualitative and quantitative analysis, and standard curves based on the molar concentration versus the peak area were established (data not shown). The results demonstrated that UPP-2 mainly consisted of xylose and glucose with a total of 88.36% in molar ratio (Fig. 1F and Table 1). There also existed arabinose (5.90%), mannose (4.26%) as well as a small amount of galactose and rhamnose.

According to previous studies, a heteropolysaccharide composed of galactose, fucose and glucose in a molar ratio of 53.51: 27.15: 19.34, and another two polysaccharides composed of galactose and fucose at approximately equal amounts were also obtained from *U. pinnatifida* (Han et al., 2016; Kim et al., 2017; Synytsya et al., 2014). The obvious differences between the present and previous studies could be attributed to two aspects: one is that the chemical composition of *U. pinnatifida* differ in the different growth conditions like regions or seasons (Boulom et al., 2014; Mak et al., 2013); the other one is that UPP-2 was one of the fractions purified from *U. pinnatifida*, it possessed unique structural characteristics but didn't represent the characteristics of crude polysaccharide perfectly.

Table 1
Monosaccharide and glycosidic bond composition of UPP-2.

Items	Molar ratio (%)
Monosaccharide composition	
Rhamnose (14.455min)	0.45
Arabinose (15.045 min)	5.90
Xylose (15.717 min)	64.55
Mannose (24.332 min)	4.26
Glucose (25.015 min)	23.81
Galactose (25.892 min)	1.03
Glycosidic bond composition	
(1→) or (1 → 6)-linkage	1.81
(1 → 2) or (1 → 4)-linkage	90.10
(1 → 3)-linkage	8.09

3.2.5. Characterization of glycosidic linkages of UPP-2

The periodate oxidation result showed that 0.9371 mol of sodium periodate was consumed per mole of hexose residue, and meanwhile 0.0181 mol of formic acid was produced. It indicated that (1 → 2) or (1 → 4)-linked glycosidic bonds in 1 mol hexose residue consumed 0.9010 mol of sodium periodate, while (1→) or (1 → 6)-linked glycosidic bonds only consumed 0.0361 mol. After Smith degradation, the residue was analyzed by GC. The presence of xylose, mannose, erythritol and glycerol in the gas chromatogram provided the existence of the above glycosidic bonds as well as (1 → 3)-linked glycosidic bonds. Based on the above data, it can be concluded that (1 → 2) or (1 → 4)-linkage were the main glycosyl linkage types (90.10% in molar ratio) of UPP-2, while (1 → 3)-linkage and (1→) or (1 → 6)-linkage only accounted for 8.09% and 1.81%, respectively (Table 1).

The glycosidic linkage types of UPP-2 were further studied by methylation, acetylation followed by GC-MS analysis. More structural information of glycosidic linkages existed in UPP-2 was identified by comparing ion fragmentations in the mass spectrum with the reference data of the CCRC spectral Database. As shown in Table 2, the molar ratio percentageof →2)-Xylp-(1→, →4)-Glcp-(1→, Xylp-(1→ and → 2,4)-Xylp-(1→ accounted for 25.26%, 23.64%, 13.08% and 10.23%, respectively, indicating that they were the main glycosidic linkages of UPP-2. According to the Hawker's equation (Hawker et al., 1991), the branch ratio of UPP-2 was calculated as 16.37%.

In order to acquire more structural information of glycoside including glycoside configuration, anomeric carbon configuration, the substitution position and branching points, as well as the species and

Table 2
Glycosidiclinkagesof methylated UPP-2.

Retention time (min)	Methylated sugar	Linkage	Molar ratio (%)
4.62	2,4-Me_2-Glcp	→3,6)-Glcp-(1→	3.21
6.15	2,3-Me_2-Araf	→5)-Araf-(1→	4.73
6.63	2,4-Me_2-Galp	→3,6)-Galp-(1→	1.54
7.30	2,3,6-Me_3-Glcp	→4)-Glcp-(1→	23.64
8.06	2,3,4,6-Me_4-GlcpNAc	GlcpA-(1→	2.69
8.29	2,3,4-Me_3-Xylp	Xylp-(1→	13.08
8.47	0-Me_0-ManpNAc	→2,3,4)-ManpA-(1→	1.39
8.58	2,3,6-Me_3-ManpNAc	→4)-ManpA-(1→	6.34
8.83	2,3-Me_2-Xylp	→4)-Xylp-(1→	7.89
8.94	3,4-Me_2-Xylp	→2)-Xylp-(1→	25.26
9.89	3-Me-Xylp	→2,4)-Xylp-(1→	10.23

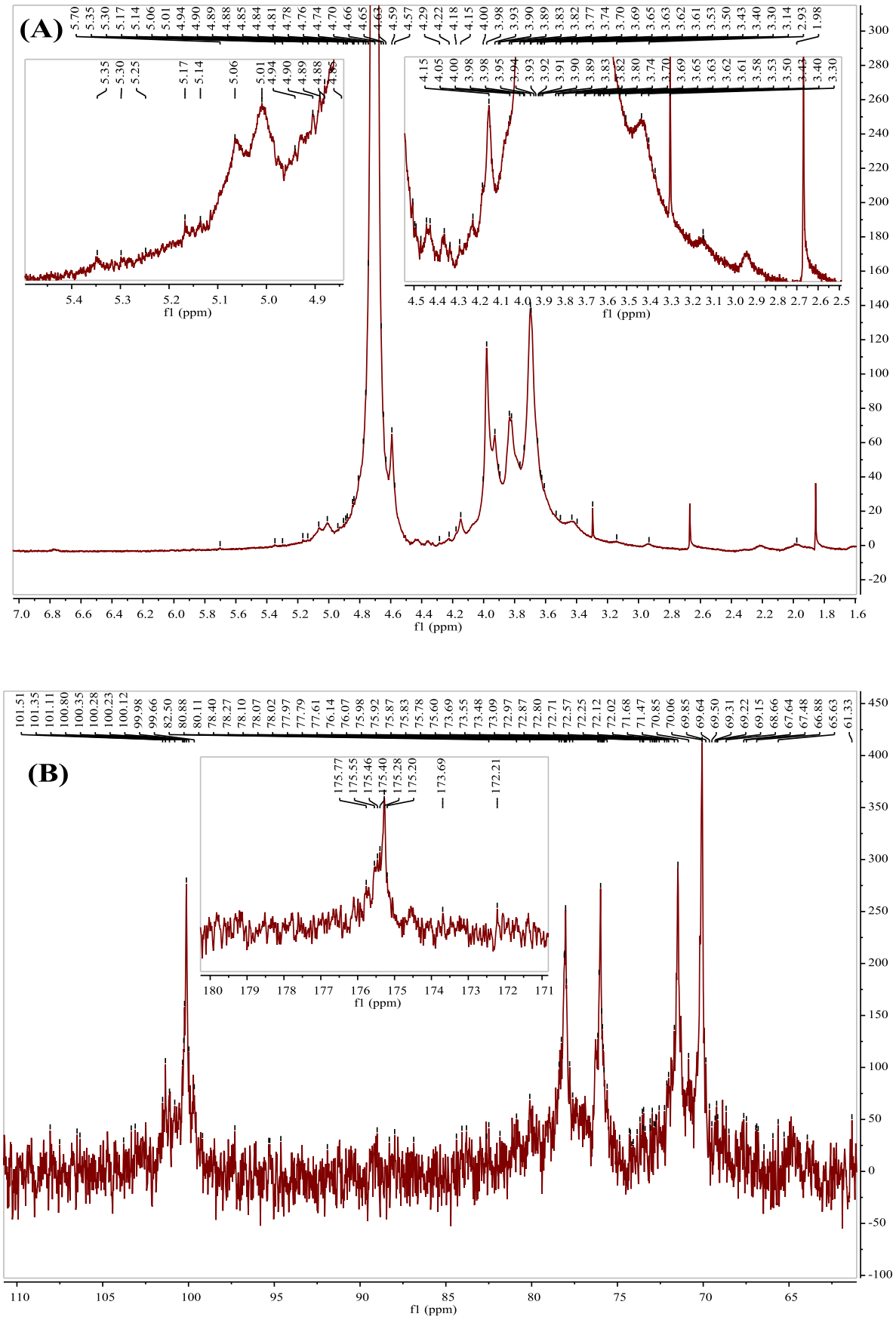

Fig. 2. ^{1}H NMR (A) and ^{13}C NMR (B) spectrum of UPP-2.

Table 3
Chemical shifts (^{1}H and ^{13}C NMR) of monosaccharide residues of UPP-2.

Sugar residue	C1/H1	C2/H2	C3/H3	C4/H4	C5/H5	C6/H6
→3,6)-α-D-Glcp-(1→	99.72/5.14	70.85/3.43	77.97/3.70	72.12/3.58	75.83/3.98	69.64/3.69
→5)-α-L-Araf-(1→	107.51/5.01	81.84/4.05	78.27/4.00	84.38/4.22	67.64/3.83,3.89	−/−
→3,6)-β-D-Galp-(1→	103.34/4.63	69.85/3.63	80.88/3.82	68.66/4.18	73.39/3.90	69.31/3.98
→4)-α-D-Glcp-(1→	99.98/5.30	78.02/3.70	73.48/4.10	77.79/3.75	72.57/3.89	60.49/3.62
α-D-GlcpNAc-(1→	91.91/4.89	55.94/3.83	72.97/3.74	71.68/3.50	72.02/3.93	175.40,23.03/1.98
α-D-Xylp-(1→	101.35/5.25	78.60/4.05	74.25/3.65	71.47/3.40	65.63/3.61	−/−
→4)-β-D-Xylp-(1→	103.78/4.57	74.31/3.37	75.02/3.64	77.35/3.74	63.93/3.37	−/−
→2)-α-D-Xylp-(1→	100.35/5.06	73.69/4.29	73.85/3.63	75.92/3.30	51.34/3.14	−/−
→2,4)-β-D-Xylp-(1→	101.51/4.66	78.07/3.53	73.09/3.69	77.61/3.82	63.94/4.15,3.43	−/−
→4)-β-D-ManpNAc-(1→	104.69/4.74	68.50/4.51	61.33/3.74	71.68/4.05	69.50/3.77	175.28/-

ratios of each residue, the ^{1}H NMR and ^{13}C NMR spectroscopy analysis of UPP-2 were carried out. The ^{1}H NMR and ^{13}C NMR spectras of UPP-2 are shown in Fig. 2. In general, the chemical shifts of the anomeric proton of pyranose in the α- and β-glycoside configurations in ^{1}H NMR spectra are usually in the range of δ 5.0–5.4 ppm and δ 4.3–4.9 ppm, respectively. Compared to ^{1}H NMR spectra, ^{13}C NMR spectra plays a more important role in the glycosidic analysis of polysaccharides for its broader chemical shift distribution (Oshima et al., 2006). And the chemical shifts in the range of δ 90–102 ppm and δ 103–110 ppm in ^{13}C NMR spectra belong to the anomeric carbon of pyranose in α- and β-glycosidic configurations, respectively (Li et al., 2015). According to the above results of monosaccharide composition and glycosidic linkage types and some previous studies (Bendahou et al., 2007; Gabrielii et al., 2000; Gao et al., 2017; Liu et al., 2014; Ren et al., 2017; Yan et al., 2017; Yuan et al., 2016), the signals in the ^{1}H NMR and ^{13}C NMR spectra were attributed and shown in Table 3. Results suggested that →2)-α-D-Xylp-(1→, →4)-α-D-Glcp-(1→, α-D-Xylp-(1→ and →2,4)-β-D-Xylp-(1→ were the main anomeric residues that constituted the main carbon chain of UPP-2, while α-D-GlcpNAc-(1→ and α-D-Xylp-(1→ were the non-reducing residues existed in the terminal of the carbon chain.

3.3. Effect of UPP-2 on RAW264.7 cell viability

As shown in Fig. 3A, UPP-2 showed significant effects on the viability of RAW264.7 cells at the test concentrations. Compared with the control group, UPP-2 exhibited an obvious promotion of macrophage proliferation in the concentration of 50–200 μg/mL ($p < 0.05$). The cell viability was about 90% of the control group at the concentration of 400 or 600 μg/mL, so the non-cytotoxic concentration range of UPP-2 was considered to be 50–600 μg/mL, while LPS showed a significant cytotoxicity to RAW264.7 cells at a concentration of 150 ng/mL ($p < 0.01$), which was consistent with the result reported by Ren et al. (2017).

3.4. Effect of UPP-2 on pinocytic capacity of RAW264.7 cells

Phagocytosis, one of the most basic defense mechanisms in the organism, is a critical basis for the ability of macrophages and neutrophils to take up and eliminate infected bacteria, viruses, and damaged cells. The enhancement of phagocytosis is a symbol of the activation of macrophages. In order to investigate whether UPP-2 could promote the activation of macrophages, the effect of UPP-2 on pinocytic activity of RAW264.7 cells was performed by neutral red reagent method. The result showed that the pinocytosis of macrophages was significantly activated by UPP-2 at the concentration of 100–800 μg/mL ($p < 0.01$, Fig. 3B). The pinocytosis of RAW264.7 cells was enhanced in a dose dependent manner at 100–600 μg/mL, but weakened at 800 mg/mL due to the slight cytotoxicity. With a 79.43% phagocytic capacity of the control group, LPS did not show the ability to promote phagocytosis of macrophages attributed to its significant cytotoxicity at 150 ng/mL.

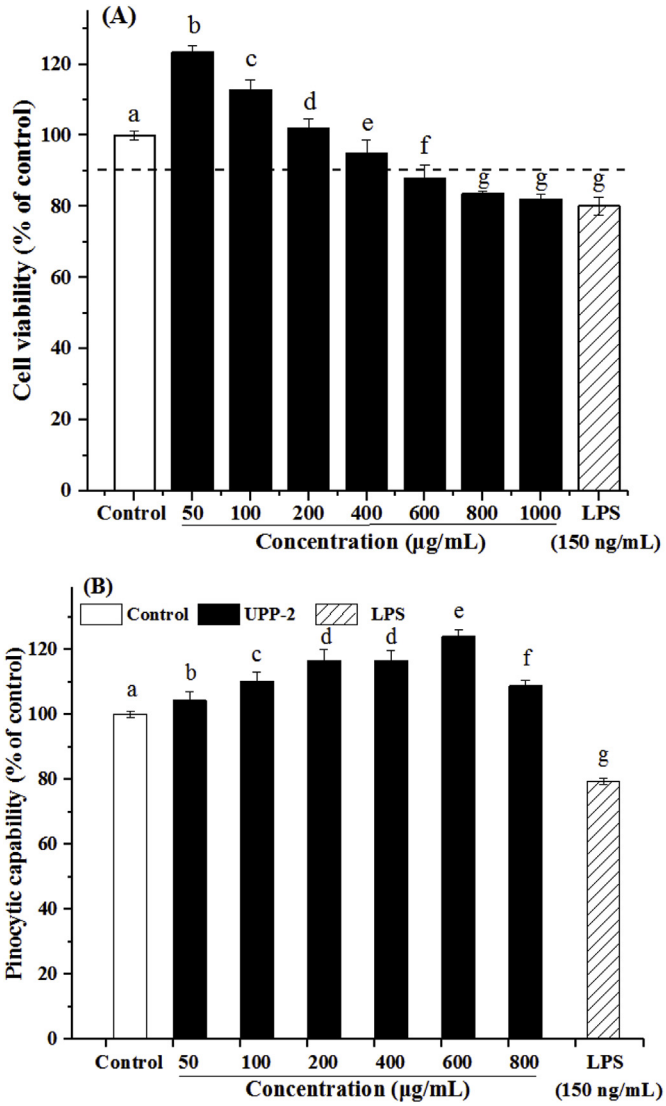

Fig. 3. The effects of UPP-2 andLPS on cell viability (A) and pinocytic capability (B) of RAW264.7 cells. Bars with different letters are significantly different ($p < 0.05$).

3.5. Effects of UPP-2 on the mRNA expression of iNOS, TNF-α, IL-6 and IL-1β in RAW264.7 cells

Nitric oxide (NO) has been recognized as an important cellular messenger or effector associated with both immune and inflammatory response. And the synthesis of NO will probably be catalyzed by iNOS when macrophages are extracellularly stimulated and activated.

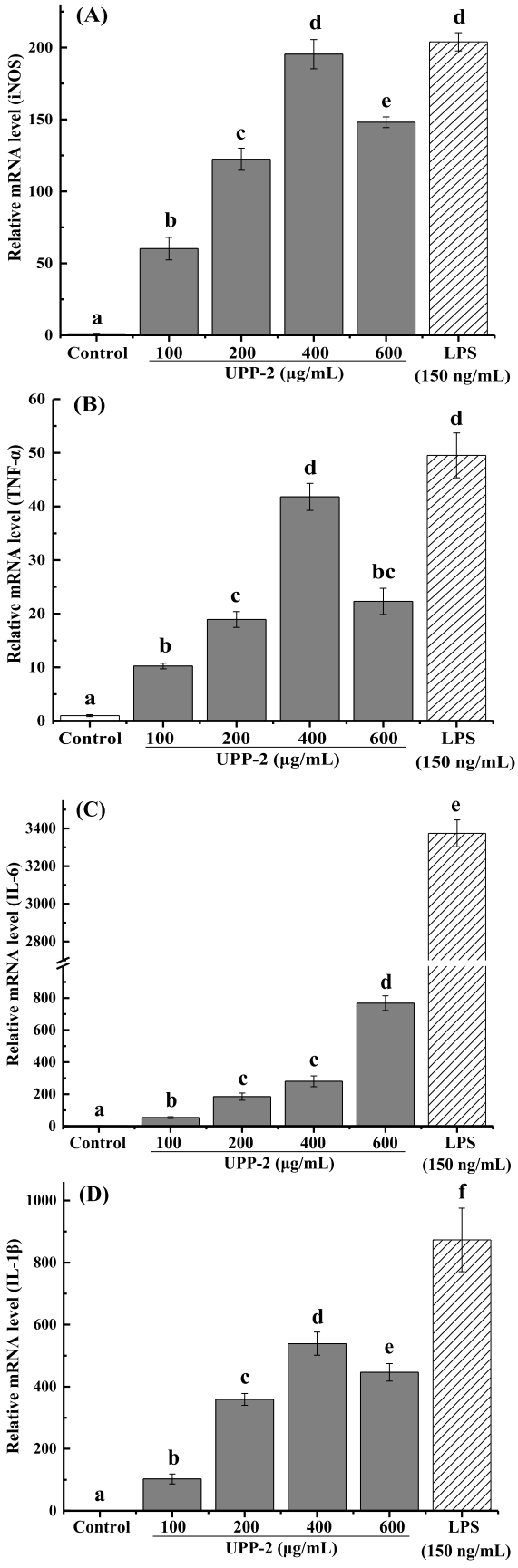

Fig. 4. Effects of UPP-2 and LPS on the mRNA expression of iNOS (A), TNF-α(B), IL-6 (C) and IL-1β (D) inRAW264.7 cells. Bars with different letters are significantly different ($p < 0.05$).

Cytokines such as TNF-α, IL-1β and IL-6, which can be secreted by activated macrophages, are the practitioners for macrophages to exert their immunomodulatory functions. In the present study, reverse transcription-quantitative real-time PCR (RT-QPCR) technique, which has been widely used in quantitative analysis of mRNA in molecular medicine, biotechnology, microbiology and diagnostics, was employed to investigate the modulatory effects of UPP-2 on the mRNA expression of iNOS, TNF-α, IL-6 and IL-1β in RAW264.7 macrophages.

As displayed in Fig. 4, the mRNA expression of iNOS, TNF-α, IL-6 and IL-1β was significantly upregulated by UPP-2 at the tested concentrations. After treated by UPP-2 at 400 μg/mL, the mRNA expression levels of iNOS, TNF-α and IL-1β were 195, 42 and 539 times of those of the negative control, respectively, showing the strongest up-regulation effects of UPP-2 on these cytokines. UPP-2 exhibited the strongest promotion effects on the mRNA expression of IL-6 at 600 μg/mL (768 times of that of the negative control). However, the mRNA expression of iNOS, TNF-α and IL-1β at 600 μg/mL obviously decreased compared with that of a concentration of 400 μg/mL, which could be ascribed to the poor state or a decrease in the number of cells caused by the slight cytotoxicity of UPP-2 at high concentration. The results above demonstrated that the promotion of mRNA expression of iNOS and TNF-α by UPP-2 (400 μg/mL) was comparable to that of LPS (150 ng/mL), while the up-regulation effects on mRNA expression of IL-6 and IL-1β were significantly weaker than that of LPS ($p < 0.05$).

3.6. Effect of UPP-2 on NO, TNF-α, IL-6 and IL-1βproduction in RAW264.7 cells

As a multifunctional cell mediator in the immune system, NO is closely related to many infectious diseases, autoimmune diseases as well as chronic degenerative diseases (Bogdan, 2001). As a host defense mechanism, macrophage-secreted cytokines including TNF-α, IL-1β, IL-6 and IL-12 are closely involved in the connection between innate and adaptive immunity (Lee et al., 2018). TNF-α plays an important role in acute local or systemic immune and inflammatory responses together with IL-6 (Li et al., 2016). IL-1β is also a key immunomodulatory molecule participating in some important cellular activities, such as cell proliferation, differentiation and cell apoptosis involved in immune system (Li et al., 2016; Yakut et al., 2015).

In this work, the secretion of NO, TNF-α, IL-6 and IL-1β in RAW264.7 cells were measured by ELISA kits. Results revealed that UPP-2 significantly promoted the secretions of NO, TNF-α and IL-6 in a dose-dependent manner within the tested concentrations (Table 4). Specifically, the highest levels of NO, TNF-α and IL-6 were 8.0, 73.1 and 188.7 times compared to those of the negative control, respectively. Compared with UPP-2, LPS unsurprisingly increased the production of NO, TNF-α and IL-6 more significantly at a concentration of 150 ng/mL. Unexpectedly, the secretion IL-1β was weakly promoted after treated with LPS or UPP-2. The result indicated that the increase of IL-1β mRNA did not result in the release of the corresponding cytokine. Likewise, honey proteins from *Ziziphus* honey could significantly affect the secretion of TNF-α, but could not affect the secretion of IL-1β (Mesaik et al., 2015). The secretion of IL-1β might be inhibited by other unknown cytokines or active substances, or might be degraded after its synthesis, while the specific reasons deserve further studies.

3.7. Structure-immunostimulatory activity relationships of UPP-2

Chemical and structural features such as molecular weight, sulfation level, monosaccharide composition and glycosidic linkages exert important influence on the immunological activity of polysaccharides. As natural macromolecules, polysaccharides generally are not directly accessible to cells. The effective combination with pattern recognition receptors (PRRs), which mainly include Toll-like receptors (such as TLR2 and TLR4), scavenger receptors, and C-type lectin-like receptors (such as Dectin-1 and mannose receptors), is critical for polysaccharides

Table 4
Effects of UPP-2 on the secretion of NO and cytokines in RAW264.7 cells.

Treatment	NO (μM)	TNF-α (pg/mL × 10)	IL-6 (pg/mL)	IL-1β (pg/mL)
Control	3.46 ± 0.49[a]	41.68 ± 1.31[a]	10.85 ± 0.71[a]	45.37 ± 1.97[a]
LPS (150 ng/mL)	32.52 ± 1.92[b]	3654.69 ± 13.23[b]	7056.14 ± 295.88[b]	62.77 ± 5.35[b]
UPP-2 (μg/mL)				
100	12.82 ± 0.90[c]	1636.73 ± 15.89[c]	37.49 ± 2.61[c]	45.02 ± 3.41[a]
200	17.29 ± 1.73[d]	1914.76 ± 54.99[d]	189.89 ± 8.06[d]	47.67 ± 0.36[a]
400	22.71 ± 0.66[e]	3067.07 ± 68.80[e]	1293.30 ± 112.74[e]	59.39 ± 3.28[bc]
600	27.77 ± 1.28[f]	3048.51 ± 92.90[e]	2047.23 ± 98.84[f]	55.35 ± 3.25[c]

[1] Data with different letters in a column are significantly different ($p < 0.05$).

to exert their immunomodulatory activities.

Molecular weight shows unspecific influence on the immunological activity of polysaccharide, but it is intrinsically related to other structural features (Ferreira et al., 2015). Monosaccharide composition of UPP-2 has an important effect on its PRRs binding capacity. It has been reported that polysaccharides with high mannose or glucose had better immune activity probably because they were easily recognized by PRRs (Figueiredo et al., 2012). Among the factions obtained in the present work, UPP-1 mainly consisted of mannose (66.73%), while UPP-2 and UPP-3 mainly contained xylose and glucose with few mannose. Results showed that the immune activity of three factions was ordered as: UPP-2 > UPP-3 > UPP-1 (data not shown). Based on these results, we hypothesized that UPP-2 exerted its immunological activity through other receptors like Toll-like receptors or complement receptors, other than mannose receptors. Besides, the high content of xylose may had a considerable contribution to the immunostimulatory activity of UPP-2. However, polysaccharides with same monosaccharide compositions but differ in structure may also activate macrophages through different receptors. For instance, a mushroom-derived β-glucan from liquid culture of *Lentinus edodes* activated macrophages via TLR-2 and Dectin-1 (Lee et al., 2008), while a β-glucan from *Amillariella mellea* activated macrophages by TLR-2 but not Dectin-1 (Yan et al., 2018).

The glycosidic linkages of UPP-2 were closely related to its immunostimulatory activity. It has been reported that sulfated α-(1 → 4)-D-glucans with α-(1 → 4)-D-Glc presented strong immunostimulatory activity while those α-(1 → 4)-D-glucans without sulfation did not exert immunostimulatory activity (Ferreira et al., 2015; Maity et al., 2014). Polysaccharides possessing a backbone of β-(1 → 4)-D-Xlyp units with attachments of α-D-GlcpNAc or α-L-Araf units were also reported to present immunostimulatory activities *in vitro* or *in vivo* (Akhtar et al., 2012; Ferreira et al., 2015; Zhou et al., 2010). In our study, UPP-2 was identified as a sulfated polysaccharide rich in →4)-α-D-Glcp-(1→, →2,4)-β-D-Xylp-(1→ as well as →4)-β-D-Xylp-(1→; Simultaneously, α-L-Araf and α-D-GlcpNAc units were also existed in UPP-2. Therefore, these glycosidic linkage units were reasonably considered as critical contributors to the immunestimulatory activity of UPP-2.

4. Conclusion

In the present study, a polysaccharide (UPP-2) with an average Mw of 1035.52 kDa was purified from *U. pinnatifida*. Without triple-helix conformational structure, UPP-2 was a low sulfated polysaccharide with relatively abundant uronic acid (13.08 ± 0.67%). Results indicated that UPP-2 mainly consisted of xylose (64.55%), glucose (23.81%), arabinose (5.90%) and mannose (4.26%). The main glycosidic linkage units of UPP-2 were identified as →2)-α-D-Xylp-(1→, →4)-α-D-Glcp-(1→, α-D-Xylp-(1→ and →2,4)-β-D-Xylp-(1→ by methylation and NMR spectroscopy analysis. UPP-2 significantly promoted the proliferation of RAW264.7 cells at low concentrations (50–200 μg/mL), and activated the pinocytosis of macrophages at the tested concentrations. Simultaneously, UPP-2 strongly upregulated the mRNA expression of iNOS, TNF-α, IL-6 and IL-1β, and significantly promoted the secretions of NO, TNF-α and IL-6 in RAW264.7 cells. In summary, the obtained results suggest that UPP-2 could be explored as a potential dietary supplement or functional food for its strong immunity enhancing function.

Conflicts of interest

The authors have no conflict of interest to declare.

Acknowledgments

This work was funded by Guangdong Special Support Program (2015TQ01N670), Pearl River S&T Nova Program of Guangzhou (201610010096), the National Natural Science Foundation of Guangdong Province (2016A030312001) and the 111 Project (B17018).

Appendix A. Supplementary data

Supplementary data to this article can be found online at https://doi.org/10.1016/j.fct.2019.03.042.

References

Akhtar, M., Tariq, A.F., Awais, M.M., Iqbal, Z., Muhammad, F., Shahid, M., Hiszczynska-Sawicka, E., 2012. Studies on wheat bran Arabinoxylan for its immunostimulatory and protective effects against avian coccidiosis. Carbohydr. Polym. 90 (1), 333–339.
Bendahou, A., Dufresne, A., Kaddami, H., Habibi, Y., 2007. Isolation and structural characterization of hemicelluloses from palm of *Phoenix dactylifera* L. Carbohydr. Polym. 68 (3), 601–608.
Bitter, T., Muir, H.M., 1962. A modified uronic acid carbazole reaction. Anal. Biochem. 4, 330–334.
Bogdan, C., 2001. Nitric oxide and the immune response. Nat. Immunol. 2 (10), 907–916.
Boulom, S., Robertson, J., Hamid, N., Ma, Q., Lu, J., 2014. Seasonal changes in lipid, fatty acid, α-tocopherol and phytosterol contents of seaweed, *Undaria pinnatifida*, in the Marlborough Sounds, New Zealand. Food Chem. 161, 261–269.
Deng, Y., Li, M., Chen, L., Chen, X., Lu, J., Zhao, J., Li, S., 2018. Chemical characterization and immunomodulatory activity of acetylated polysaccharides from *Dendrobium devonianum*. Carbohydr. Polym. 180, 238–245.
Dubois, M., Gilles, K., Hamilton, J.K., Rebers, P.A., Smith, F., 1951. A colorimetric method for the determination of sugars. Nature 168 (4265), 167.
Faggio, C., Morabito, M., Minicante, S.A., Piano, G.L., Pagano, M., Genovese, G., 2015. Potential use of polysaccharides from the brown alga *Undaria pinnatifida* as anticoagulants. Braz. Arch. Biol. Technol. 58 (5), 798–804.
Ferreira, S.S., Passos, C.P., Madureira, P., Vilanova, M., Coimbra, M.A., 2015. Structure-function relationships of immunostimulatory polysaccharides: a review. Carbohydr. Polym. 132, 378–396.
Figueiredo, R.T., Bittencourt, V.C.B., Lopes, L.C.L., Sassaki, G., Barreto-Bergter, E., 2012. Toll-like receptors (TLR2 and TLR4) recognize polysaccharides of Pseudallescheria boydii cell wall. Carbohydr. Res. 356, 260–264.
Gabrielii, I., Gatenholm, P., Glasser, W.G., Jain, R.K., Kenne, L., 2000. Separation, characterization and hydrogel-formation of hemicellulose from aspen wood. Carbohydr. Polym. 43 (4), 367–374.
Gao, J., Lin, L., Sun, B., Zhao, M., 2017. Comparison study on polysaccharide fractions from *Laminaria japonica*: structural characterization and bile acid binding capacity. J. Agric. Food Chem. 65 (44), 9790–9798.
Han, Y., Wu, J., Liu, T., Hu, Y., Zheng, Q., Wang, B., Lin, H., Li, X., 2016. Separation, characterization and anticancer activities of a sulfated polysaccharide from *Undaria pinnatifida*. Int. J. Biol. Macromol. 83, 42–49.
Hawker, C.J., Lee, R., Frechet, J., 1991. One-step synthesis of hyperbranched dendritic polyesters. J. Am. Chem. Soc. 113 (12), 4583–4588.
Hifney, A.F., Fawzy, M.A., Abdel-Gawad, K.M., Gomaa, M., 2016. Industrial optimization of fucoidan extraction from *Sargassum* sp. and its potential antioxidant and

emulsifying activities. Food Hydrocolloids 54, 77–88.
Ji, D.S., You, L.J., Ren, Y.L., Wen, L.R., Zheng, G.Q., 2017. Protective effect of polysaccharides from Sargassum fusiforme against UVB-induced oxidative stress in HaCaT human keratinocytes. J Funct. Foods 36, 332–340.
Jiao, G., Yu, G., Zhang, J., Ewart, H., 2011. Chemical structures and bioactivities of sulfated polysaccharides from Marine Algae. Mar. Drugs 9 (12), 196–223.
Jin, F., Jia, L., Tu, Y., 2015. Structural analysis of an acidic polysaccharide isolated from white tea. Food Sci. Biotechnol. 24 (5), 1623–1628.
Kim, W.J., Choi, J.W., Jang, W.J., Kang, Y., Lee, C.W., Synytsya, A., Park, Y.I., 2017. Low-molecular weight mannogalactofucans prevent herpes simplex virus type 1 infection *via* activation of Toll-like receptor 2. Int. J. Biol. Macromol. 103, 286–293.
Lee, J.Y., Kim, J.Y., Lee, Y.G., Rhee, M.H., Hong, E.K., Cho, J.Y., 2008. Molecular mechanism of macrophage activation by exopolysaccharides from liquid culture of *Lentinus edodes*. J. Microb. Biotechnol. 18 (2), 355–364.
Lee, S.J., Lee, H.S., Kim, S.Y., Shin, K., 2018. Immunostimulatory and anti-metastatic activity of polysaccharides isolated from byproducts of the corn starch industry. Carbohydr. Polym. 181, 911–917.
Li, C., You, L.J., Fu, X., Huang, Q., Yu, S., Liu, R.H., 2015. Structural characterization and immunomodulatory activity of a new heteropolysaccharide from *Prunella vulgaris*. Food Funct 6 (5), 1557–1567.
Li, L., Li, H., Qian, J., He, Y., Zheng, J., Lu, Z., Xu, Z., Shi, J., 2016. Structural and immunological activity characterization of a polysaccharide isolated from *Meretrix meretrix* linnaeus. Mar. Drugs 14 (12), 6.
Liang, B., Jin, M., Liu, H., 2011. Water-soluble polysaccharide from dried *Lycium barbarum* fruits: isolation, structural features and antioxidant activity. Carbohydr. Polym. 83 (4), 1947–1951.
Lin, L., Zhuang, M., Zou, L., Lei, F., Yang, B., Zhao, M., 2012. Structural characteristics of water-soluble polysaccharides from *Rabdosia serra* (MAXIM.) HARA leaf and stem and their antioxidant capacities. Food Chem. 135 (2), 730–737.
Liu, J., Wen, X., Kan, J., Jin, C., 2014. Structural characterization of two water-soluble polysaccharides from Black Soybean (*Glycine max* (L.) Merr.). J. Agric. Food Chem. 63 (1), 225–234.
Livak, K.J., Schmittgen, T.D., 2001. Analysis of relative gene expression data using real-time quantitative PCR and the $2^{-\Delta\Delta CT}$ method. Methods 25 (4), 402–408.
Lucassen, G.W., van Veen, G.N.A., Jansen, J.A.J., 1998. Band analysis of hydrated human skin stratum corneum attenuated total reflectance fourier transform infrared spectra *in vivo*. J. Biomed. Opt. 3 (3), 267–280.
Maity, P., Pattanayak, M., Maity, S., Nandi, A.K., Sen, I.K., Behera, B., Maiti, T.K., Mallick, P., Sikdar, S.R., Islam, S.S., 2014. A partially methylated mannogalactan from hybrid mushroom *pfle 1p*: purification, structural characterization, and study of immunoactivation. Carbohydr. Res. 395, 1–8.
Mak, W., Hamid, N., Liu, T., Lu, J., White, W.L., 2013. Fucoidan from New Zealand *Undaria pinnatifida*: monthly variations and determination of antioxidant activities. Carbohydr. Polym. 95 (1), 606–614.
Manrique, G.D., Lajolo, F.M., 2002. FT-IR spectroscopy as a tool for measuring degree of methyl esterification in pectins isolated from ripening papaya fruit. Postharvest Biol. Technol. 25 (1), 99–107.
Mesaik, M.A., Dastagir, N., Uddin, N., Rehman, K., Azim, M.K., 2015. Characterization of immunomodulatory activities of honey glycoproteins and glycopeptides. J. Agric. Food Chem. 63 (1), 177–184.
Ngo, D., Kim, S., 2013. Sulfated polysaccharides as bioactive agents from marine algae. Int. J. Biol. Macromol. 62, 70–75.
Oshima, H., Kimura, I., Izumori, K., 2006. Synthesis and structure analysis of novel disaccharides containing D-psicose produced by endo-1,4-β-D-xylanase from *Aspergillus sojae*. J. Biosci. Bioeng. 101 (3), 280–283.
Phull, A., Majid, M., Haq, I., Khan, M.R., Kim, S.J., 2017. *In vitro* and *in vivo* evaluation of anti-arthritic, antioxidant efficacy of fucoidan from *Undaria pinnatifida* (Harvey) Suringar. Int. J. Biol. Macromol. 97, 468–480.
Ren, Y., Zheng, G., You, L., Wen, L., Li, C., Fu, X., Zhou, L., 2017. Structural characterization and macrophage immunomodulatory activity of a polysaccharide isolated from *Gracilaria lemaneiformis*. J. Funct. Foods 33, 286–296.
Shen, C., Zhang, T., Zhang, W., Jiang, J., 2016. Anti-inflammatory activities of essential oil isolated from the calyx of *Hibiscus sabdariffa L*. Food Funct 7 (10), 4451–4459.
Singleton, V.L., Orthofer, R., Lamuela-Raventos, R.M., 1999. Analysis of total phenols and other oxidation substrates and antioxidants by means of Folin-Ciocalteu reagent. Packer, L. (Ed.), Methods Enzymol. 299 (1), 152–178.
Song, K., Ha, S.J., Lee, J., Kim, S., Kim, Y.H., Kim, Y., Hong, S.P., Jung, S.K., Lee, N.H., 2015. High yield ultrasonication extraction method for *Undaria pinnatifida* sporophyll and its anti-inflammatory properties associated with AP-1 pathway suppression. LWT - Food Sci. Technol. (Lebensmittel-Wissenschaft -Technol.) 64 (2), 1315–1322.
Synytsya, A., Bleha, R., Synytsya, A., Pohl, R., Hayashi, K., Yoshinaga, K., Nakano, T., Hayashi, T., 2014. Mekabu fucoidan: structural complexity and defensive effects against avian influenza A viruses. Carbohydr. Polym. 111, 633–644.
Vishchuk, O.S., Ermakova, S.P., Zvyagintseva, T.N., 2013. The fucoidans from brown algae of Far-Eastern seas: anti-tumor activity and structure-function relationship. Food Chem. 141 (2), 1211–1217.
Xu, X., Yan, H., Zhang, X., 2012. Structure and immuno-stimulating activities of a new heteropolysaccharide from *Lentinula edodes*. J. Agric. Food Chem. 60 (46), 11560–11566.
Yakut, E., Jakobs, C., Peric, A., Michel, G., Baal, N., Bein, G., Bruene, B., Hornung, V., Hackstein, H., 2015. Extracorporeal photopheresis promotes IL-1β production. J. Immunol. 194 (6), 2569–2577.
Yan, J., Han, Z., Qu, Y., Yao, C., Shen, D., Tai, G., Cheng, H., Zhou, Y., 2018. Structure elucidation and immunomodulatory activity of a β-glucan derived from the fruiting bodies of *Amillariella mellea*. Food Chem. 240, 534–543.
Yan, J., Wang, Y., Qiu, W., Wu, L., Ding, Z., Cai, W., 2017. Purification, structural characterization and bioactivity evaluation of a novel proteoglycan produced by *Corbicula fluminea*. Carbohydr. Polym. 176, 11–18.
Ye, Y.H., Ji, D.S., You, L.J., Zhou, L., Zhao, Z.G., Brennan, C., 2018. Structural properties and protective effect of *Sargassum fusiforme* polysaccharides against ultraviolet B radiation in hairless Kun Ming mice. J. Func Foods 43, 8–16.
Yu, X., Liu, Y., Wu, X., Liu, L., Fu, W., Song, D., 2017. Isolation, purification, characterization and immunostimulatory activity of polysaccharides derived from *American ginseng*. Carbohydr. Polym. 156, 9–18.
Yuan, Y., Wang, Y., Jiang, Y., Prasad, K.N., Yang, J., Qu, H., Wang, Y., Jia, Y., Mo, H., Yang, B., 2016. Structure identification of a polysaccharide purified from *Lycium barbarium* fruit. Int. J. Biol. Macromol. 82, 696–701.
Zhang, H., Wang, J., Nie, S., Wang, Y., Cui, S.W., Xie, M., 2015a. Sulfated modification, characterization and property of a water-insoluble polysaccharide from *Ganoderma atrum*. Int. J. Biol. Macromol. 79, 248–255.
Zhang, W., Oda, T., Yu, Q., Jin, J., 2015b. Fucoidan from *Macrocystis pyrifera* has powerful immune-modulatory effects compared to three other fucoidans. Mar. Drugs 13 (3), 1084–1104.
Zhang, Y., Liu, D., Fang, L., Zhao, X., Zhou, A., Xie, J., 2018. A galactomannoglucan derived from *Agaricus brasiliensis*: purification, characterization and macrophage activation via MAPK and IκB/NFκB pathways. Food Chem. 239, 603–611.
Zhou, S., Liu, X., Guo, Y., Wang, Q., Peng, D., Cao, L., 2010. Comparison of the immunological activities of arabinoxylans from wheat bran with alkali and xylanase-aided extraction. Carbohydr. Polym. 81 (4), 784–789.